Evolution of
Mylonitic Microfabrics

Insights from See-Through Deformation of Norcamphor

© by Marco Herwegh, Mark Handy & Renée Heilbronner

Glossary Goals Content Overview Experiments Microfabric Evolution

Glossary (Use back button on browser to return to previous page)

C-Axis Cross Girdle
The skeletal outline of all c-axes in a pole figure comprises two girdles at a low angle to each other. Together, these girdles form a cross in a pole figure.

C-Axis Point Maxima
A concentration of c-axes at point maxima within the pole figure.

C-Axis Single Girdle
A concentration of c-axes along a great circle within a pole figure.

CIP (computer integrated polarization microscopy)
This technique allows one to represent the c-axis position of each pixel with a characteristic color. Therefore, the microfabric can be presented as c-axis orientation images (COIs) in which the CPO can be directly inferred from the actual colors of grains and domains. For more detailed information about CIP, see Panozzo-Heilbronner, R. & Pauli, C. 1993. Integrated spatial and orientation analysis of quartz c-axes by computer-aided microscopy. J. Struct. Geol. , 15, 369-383.

CPO (Crystallographic Preferred Orientaion)
The tendency of crystallographic axes to occupy a specific orientation with respect to external fabric coordinates; a non-random distribution of c-axes in a pole figure (e.g. along great circles).

Dislocation Creep
Deformation mechanism involving the glide and climb of dislocations within the crystal lattice.

Domains
Groups of grains that have the same CPO and/or SPO.

Easy Glide Orientation
Special orientations of intracrystalline glide planes for which the resolved shear stress on the glide plane is maximized.

Fracturing
The nucleation and growth of cracks

Glide Induced Vorticity
Rotation of c-axes associated with intracrystalline gliding (see Lister, G.S. 1982. A vorticity equation for lattice reorientation during plastic deformation. Tectonophysics , 82, 351-366).

GBM (grain boundary migration)
Movement of grain boundaries involving the growth of one grain and consumption of another. In our experiments, GBM is assumed to be driven primarily by the reduction of internal strain energy, i.e. the stored energy.

HT-HS
High Temperature - High Strain Rate Experiments.

HT-LS
High Temperature - Low Strain Rate Experiments.

Instanteneous Stretching Direction
Direction of incremental extension at 45° with respect to the shear zone boundary in simple shear.

IT-HS
Intermediate Temperature - High Strain Rate Experiments.

LT-HS
Low Temperature - High Strain Rate Experiments.

Marker Analysis
A computer program which allows one to calculate strain distribution within a deforming aggregate based on the digitized positions of tiny marker particles within the aggregate. For more information see Bons, P., Jessell, M.W. & Passchier, C.W. 1993. The analysis of progressive deformation in rock analogues. J. Struct. Geol. , 15, 403-412.

Microfabric
The Microfabric comprises the microstructure and the texture of a material.

Microstructure
Microstructure comprises the geometric elements of the microfabric e.g. grain size and grain shape.

PAROR (Particle Orientation)
This computer program calculates the orientation distribution of particles´ long axes and short/long axis ratios. For further information see Panozzo, R. 1983. Two-dimensional analysis of shape-fabric using projections of digitized lines in a plane. Tectonophysics, 95, 279-294.

Rigid Body Rotation
Rotation of grains without internal deformation. This mechanism occurs especially in grains which are unfavorably oriented for intracrystalline deformation.

Rotational Mechanisms
Mechanisms that rotate grains´ crystallography into orientations which are favorable for intracrystalline glide. Such mechanisms include rigid body rotation, glide induced vorticity and subgrain rotation.

SPO
Shape Preferred Orientation; A non-random distribution of grain shapes.

Spontaneous Nucleation
The sudden appearance of new grains within an aggregate. Such nucleation is inferred to involve rapid subgrain rotation.

Steady State
Strain invariance of the microfabric on the sample scale.

Subgrain Rotation Recr .
The formation of crystallographically distinct parts of grains (subgrains) via the climb of dislocations into polygonally arranged walls.

SURFOR (Surface Orientation)
This computer program calculates the orientation distribution of surfaces. For further information see Panozzo, R. 1984:. Two-dimensional strain from the orientation of lines in a plane. J. Struct. Geol. , 6, 215-221.

SZB
Shear Zone Boundary

Texture
Preferred orientation of crystallographic axes in the sample.

Glossary Home

Goals

Microfabrics contain important information about the physical conditions, the kinematics and the processes of deformation. The kinematics of deformation (i.e., the shear sense), for example, are often inferred from the asymmetry of microstructural and textural features in deformed rocks. In order to gain a better understanding of kinematic indicators and the deformational behavior of minerals at different physical conditions, researchers have studied the mechanical properties and microfabrics of most common rock-forming minerals (e.g., quartz, calcite, feldspar, olivine). The study of naturally deformed rocks, experimental rock deformation, and computer modeling have all played complementary roles in improving our knowledge of mineral physics.

We chose an experimental approach involving the deformation of polycrystalline norcamphor in a see-through, Means-Urai deformation apparatus under simple shear conditions. The main advantage of this method is that it allows continuous observation of the microfabric evolution during progressive deformation. We monitored this evolution with photographs, video tapes and computer integrated polarization microscopy (CIP, see Panozzo Heilbronner, R. & Pauli, C. 1993. Integrated spatial and orientation analysis of quartz c-axes by computer-aided microscopy. J. Struct. Geol. 15, 369-383). With CIP, the c-axis orientations are visualized directly with specific reference colors. Strain was calculated with help of passive marker particles and the computer program Marker Analysis (Bons, P., Jessell, M.W. & Passchier, C.W. 1993. The analysis of progressive deformation in rock analogues. J. Struct. Geol. 15, 403-412.) This allowed us to relate the microstructure, the texture and the localization of strain in each experiment.

If desired, more information about the applied techniques and the results of these experiments can be found in:

Herwegh, M. 1996. Microfabric Evolution in Monomineralic Mylonites: An Experimental Approach Using See-Through Analogue Materials. Unpublished Ph.D. thesis, University of Berne.

Herwegh, M. & Handy, M.R. 1996. The Evolution of High Temperature Mylonitic Microfabrics: Evidence from Simple Shearing of a Quartz Analogue (Norcamphor). J. Struct. Geol., 18, 689-710.

Herwegh, M. & Handy, M. R. 1998. The origin of shape preferred orientations in mylonite: inferences from in-situ experiments on polycrystalline norcamphor. J. Struct. Geol. 20, 681-694.

Herwegh, M., Handy, M.R. & Panozzo Heilbronner, R. 1997. Temperature and Strain Rate Dependent Microfabric Evolution in Monomineralic Mylonite: Evidence from In Situ Deformation of Norcamphor. Tectonophysics 280, 83-106.

Herwegh, M., Handy, M.R. & Panozzo Heilbronner, R. 1999. Evolution of mylonitc microfabrics (EMM), a computer application for educational purposes. Tectonophysics 303, 141-146.

Panozzo Heilbronner, R., & Herwegh, M. 1997. Time slicing, an image processing technique to visualize temporal development of fabrics. J. Struct. Geol. 19, 861-874.

Glossary Home

Content

The interactive computer program "Evolution of Mylonitic Microfabrics (EMM)" was created as a File MakerPro 3.0 application. The program comprises graphics, animations and explanations of various aspects of microfabric evolution. The program has several different levels between which the reader can readily move by clicking on the corresponding buttons. Information about special terms used in EMM can be obtained simply by clicking on the Glossary button in the upper right hand corner of the page.

The web version of this programm was assembled by Mark Jessell and any problems with the format are probably his fault. Mark is greatfully acknwoldeged for doing a great job.

Starting from the main MENU, the program is divided into five submenues: (1) **Goals**, (2) **Content**, (3) **Overview**, (4) **Experiments** and (5) **Microfabric Evolution:**

(1) Goals
presenting the principle goals and techniques applied in this experimental study (Goals).

(2) Content
listing the EMM computer program (Content)

(3) Overview
giving a complete listing of the different levels of the program and the paths by which these levels can be reached (Overview).

(4) Experiments
representing a series of norcamphor experiments which were carried out at different strain rate and temperature conditions:

HT-LS: High Temperature - Low Strain Rate
HT-HS: High Temperature - High Strain Rate
IT-HS: Intermediate Temperature - High Strain Rate
LT-HS: Low Temperature - High Strain Rate

The submenu Experiments contains information about norcamphor as a rock analogue material, the experimental configuration and the experimental CONDITIONS. The database and the description of the different experiments can be found in the individual subgroups (HT-LS, HT-HS, IT-HS, LT-HS)., These deal with the following aspects:

- Animations and explanations of the microfabric evolution
- Diagram of changes in area proportions of specific c-axis orientations
- Diagram of strain dependent changes in the mechanism activities
- Animation and explanation of the textural evolution
- Animation and explanation of strain dependent changes in grain size
- Particle orientations of grains and domains (PAROR)
- Surface orientations of grains and domains (SURFOR)
- Animation of the strain distribution pattern
- Animation of the distribution of high strain zones

To compare microfabric elements from one experiment with those of another, click on buttons at the

bottom of the page. This allows one to switch directly to the corresponding page of another experiment.

(5) Microfabric Evolution

This chapter contains the general evolution of TEXTURE and MICROSTRUCTURE. These are explained in detail and summarized in SYNTHESIS.

The TEXTURE subchapter deals with:

- Textures at the different experimental conditions
- Changes in obliquity of c-axis cross and single girdles with strain
- Strain dependence of the opening angles of the c-axis cross girdles
- C-axis rotation paths
- Changes in c-axis inclinations
- Changes in c-axis azimuths
- Stabilities of c-axis orientations
- Preservation of steady state textures

The following points are treated in the MICROSTRUCTURE subchapters (GRAIN/DOMAIN SIZE, SPO & LOCALIZATION) :
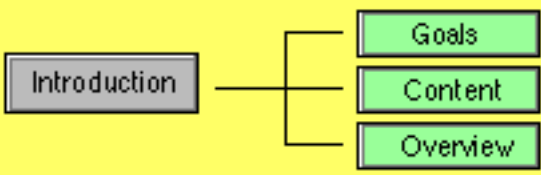
- Temperature and strain rate dependent changes in grain size
- Temperature and strain rate dependent changes in domain width
- Evolution of grain SPO
- Evolution of domain SPO
- Strain distribution patterns
- Occurrence of microshear zones
- Relationship between microshear zones and microstructure
- Formation of microshear zones
- History of microshear zones
- Rotation diagrams of microshear zones
- Relationship between microshear zones and SPOs
- General localization behavior

The SYNTHESIS summarizes the microfabric evolution to steady state on different scales.

Overview (Active links in green)

Evolution of Monomineralic Mylonitic Microfabrics
Insights from See-Through Deformation of Norcamphor

MENU

Introduction
- Goals
- Content
- Overview

Experiments
- Norcamphor
- Configuration
- Conditions
- HT-LS
- HT-HS*
- IT-HS
- LT-HS
  - Microfabric Ev.
  - Area Proportions
  - Mechanism Activities
  - Textures
  - Grain Areas
  - PAROR
  - SURFOR
  - Strain Distribution
  - High Strain Zones

Microfabric Evolution
- Texture
  - All Textures
  - Textural Obliquity
  - Opening Angle
  - C-Axis Rotation
  - C-Axis Inclination
  - C-Axis Azimuth
  - C-Axis Stabilities
  - Steady State T.
- Microstructure
  - Grain/Domain Size
    - Grain Size
    - Domain Width
  - SPO & Local.
    - Grain SPO
    - Domain SPO
    - Strain Distribution
    - Microshear Zones
    - MSZ-Microstructure
    - MSZ Formation
    - MSZ History
    - MSZ Rotation
    - SPO & MSZ
    - General Localization
- Synthesis
  - Microfabric Ev.
  - Scales
  - Steady State

Glossary Experiments

Experimental Conditions

	HT-LS	HT-HS	IT-HS	LT-HS
T (°C)	25	25	10	4
T_h (T/T_m)	0.81	0.81	0.77	0.76
shear strain rate (s^{-1})	4.0 x 10-5	5.5 x 10-4	5.5 x 10- 4	5.5 x 10-4
shear strain (γ)	7.9	10.5	9	5
exp. duration (hrs)	55	5 1/4	4 1/2	2 1/2

HT-LS: high temperature, low strain rate

HT-HS: high temperature, high strain rate

IT-HS: intermediate temperature, high strain rate

LT-HS: low temperature, high strain rate

Configuration
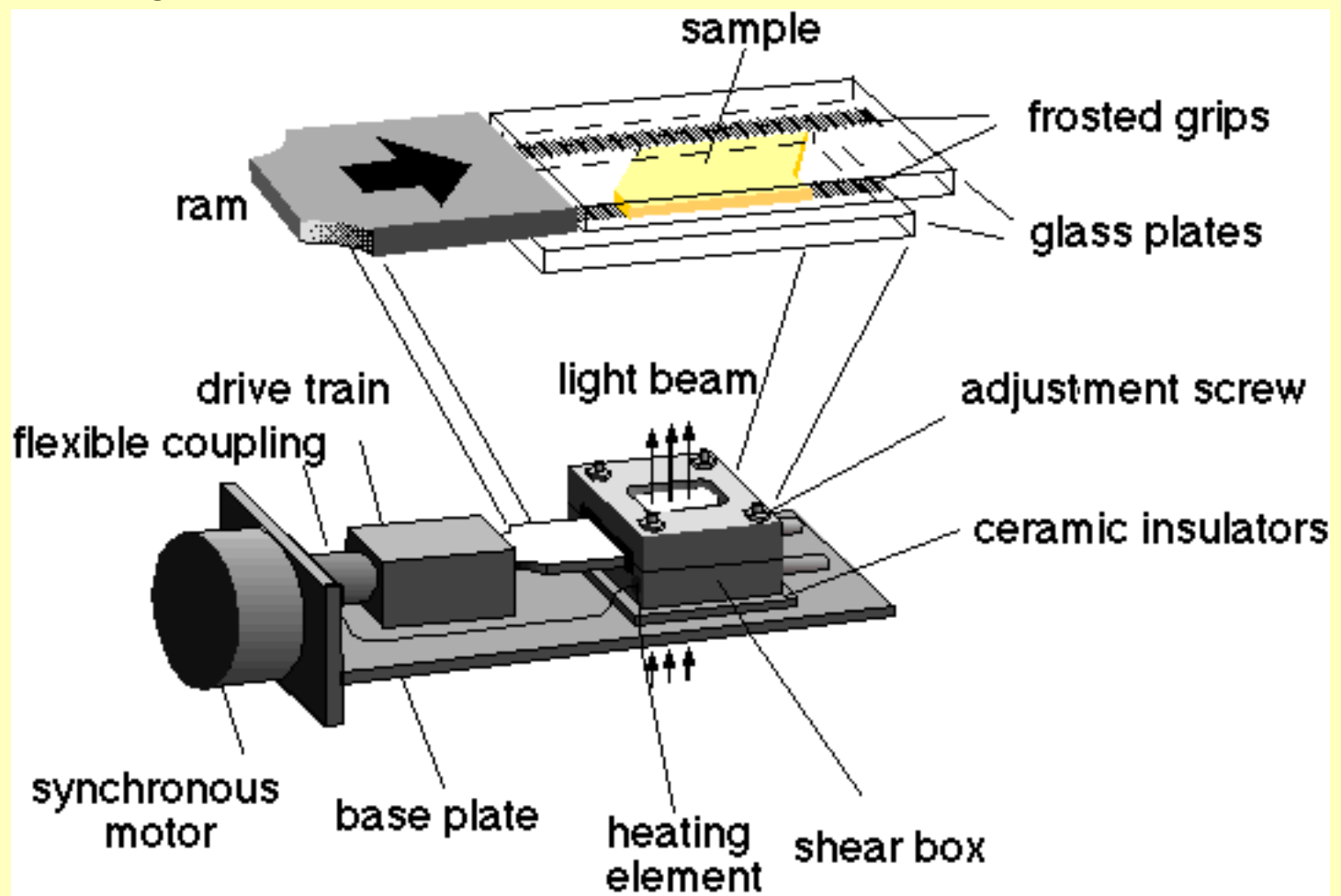
We placed the Urai-Means deformation rig on a photomacroscope and then continuously monitored the microstructure with video or photographs. Each motor turns at a set number of rpm.

A synchronous motor attached to the end of the rig drives the ram at a constant velocity into the deformation cell. The velocity of the ram can be varied by changing the synchronous motor.

The deformation cell itself comprises two glass plates with frosted grips and the sample material in between. The ram pushes the upper glass plate relative to the lower one, resulting in a simple shear deformation of the rock analogue material.

Externally controlled heating elements allow one to vary the temperature in the deformation cell.

Glossary Home

Texture:

- Texture

Microstructure:

- Grain Size
- Domain Size
- SPO & Localisation

Synthesis:

- Microfabric Evolution
- Scales
- Steady State

LT-HS Microfabric Evolution
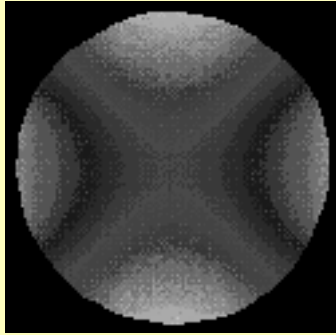
First transient stage ($0<\gamma<2$):

Initial deformation involves limited crystal plasticity (undulose extinction) and rigid body rotation accommodated at grain boundaries by dynamic recrystallization. These processes are not able to maintain strain compatibility, however, as evidenced by the nucleation and growth of fractures with progressive strain. The traces of incipient fractures are parallel to the incremental compression direction (135°). These fractures open parallel to the incremental stretching direction (45°). With increasing strain, the small fractures either rotate synthetically and close, or they interconnect to form large dilatational veins which transect the entire sample.

Second transient stage ($\gamma>2$):

Subgrain rotation recrystallization is more pronounced between the two big veins.

Steady state :

No steady state microfabric was attained on the sample scale, presumably due to dilatancy along the big veins.

IT-HS Microfabric Evolution
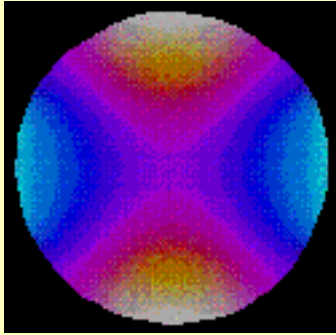
First transient stage ($0 < \gamma < 2$):

The volume proportions of yellow and magenta grains increase at the expense of the proportions of bright blue and dark blue grains. This is attributed to subgrain rotation and glide induced vorticity, both of which rotate the grains´ crystallography into orientations that are more favourable for intracrystalline gliding. Note the formation of a stable, oblique grain SPO at angles of about 60° with respect to the SZB.

Second transient stage ($2 < \gamma < 6$):

The increase in areal proportion of yellow grains is attributed to a combination of subgrain rotation and grain boundary migration recrystallization. The coalescence of yellow grains leads to the formation of a microfabric comprising yellow and magenta domains. Along the SZB, few small fractures appear which grow subparallel to the incremental stretching direction.

Steady state ($\gamma > 6$):

The areal proportion of yellow and magenta grains is strain invariant on the sample scale. On the grain scale, however, a cyclical behavior of consumption and growth of individual grains. This behaviour is identical to that of steady state in the HT-LS experiments.

Analogy:

The microfabric is very similar to that to natural quartz mylonite deformed under greenschist facies conditions.

HT-HS Microfabric Evolution
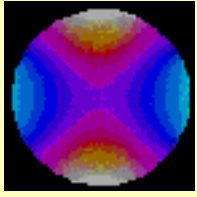
First transient stage ($\gamma < 2$):
As in the HT-LS experiments, changes in interference colors result from highly active rotational mechanisms which orient grains´ crystallography more favourably for intracrystalline gliding.

Second transient stage ($2<\gamma<8$):
Yellow grains grow at the expense of all other grain orientations via grain boundary migration. This results in the formation of a domainal microfabric consisting of yellow and magenta grains.

Steady state ($\gamma > 8$, not reported in the animation):
A steady state microfabric is maintained in the same manner as in the HT-LS experiments.

Analogy:
The microfabric shows a high analogy to natural quartz mylonites deformed under upper greenschist to amphibolite facies conditions.

HT-LS Microfabric Evolution

First transient stage (0<γ<1.5):
Blue and violet grains disappear whereas the volume proportions of yellow and magenta grains increase. We attribute this behavior to continuous reorientation of the grains´ crystallography into orientations that are favourable for intracrystalline gliding (i.e., easy glide orientations).
Note the formation of a stable, oblique grain SPO at angles of about 60° with respect to the SZB.

Second transient stage (1.5<γ<6):
Grain boundary migration recrystallization is the predominant grain scale mechanism. The area proportion of the yellow grains, for example, increases significantly at the expense of the area proportion of magenta grains. This behavior leads to a strongly domainal microfabric consisting of yellow and magenta domains.

Steady state (γ>6):
The area proportion of yellow and magenta grains is strain invariant on the sample scale. On the grain scale, however, one can observe cyclical consumption and growth of individual grains (e.g., see magenta grains in the lower left hand corner).

Analogy:
This steady state microfabric in norcamphor is very similar to that of natural quartz mylonites deformed under upper greenschist to amphibolite facies conditions (see Fig. 12 in Herwegh & Handy, 1996)

Norcamphor C$_7$H$_{10}$O

- melting point (Tm): 92-98°C
- optical properties: uniaxial negative
- crystallography: hexagonal?
- previously used as rock analogue by:

-Bons (1993)

-Herwegh (1996)

-Herwegh & Handy (1996)

-Herwegh et al. (1997)

-Herwegh & Handy (1998)

-Panozzo Heilbronner & Herwegh (1997)

-Herwegh et al. (1999)

Glossary Home

Experiments

- HT-LS
- HT-HS
- IT-HS
- LT-HS

Background

- Norcamphor
- Configuration
- Conditions

Textures
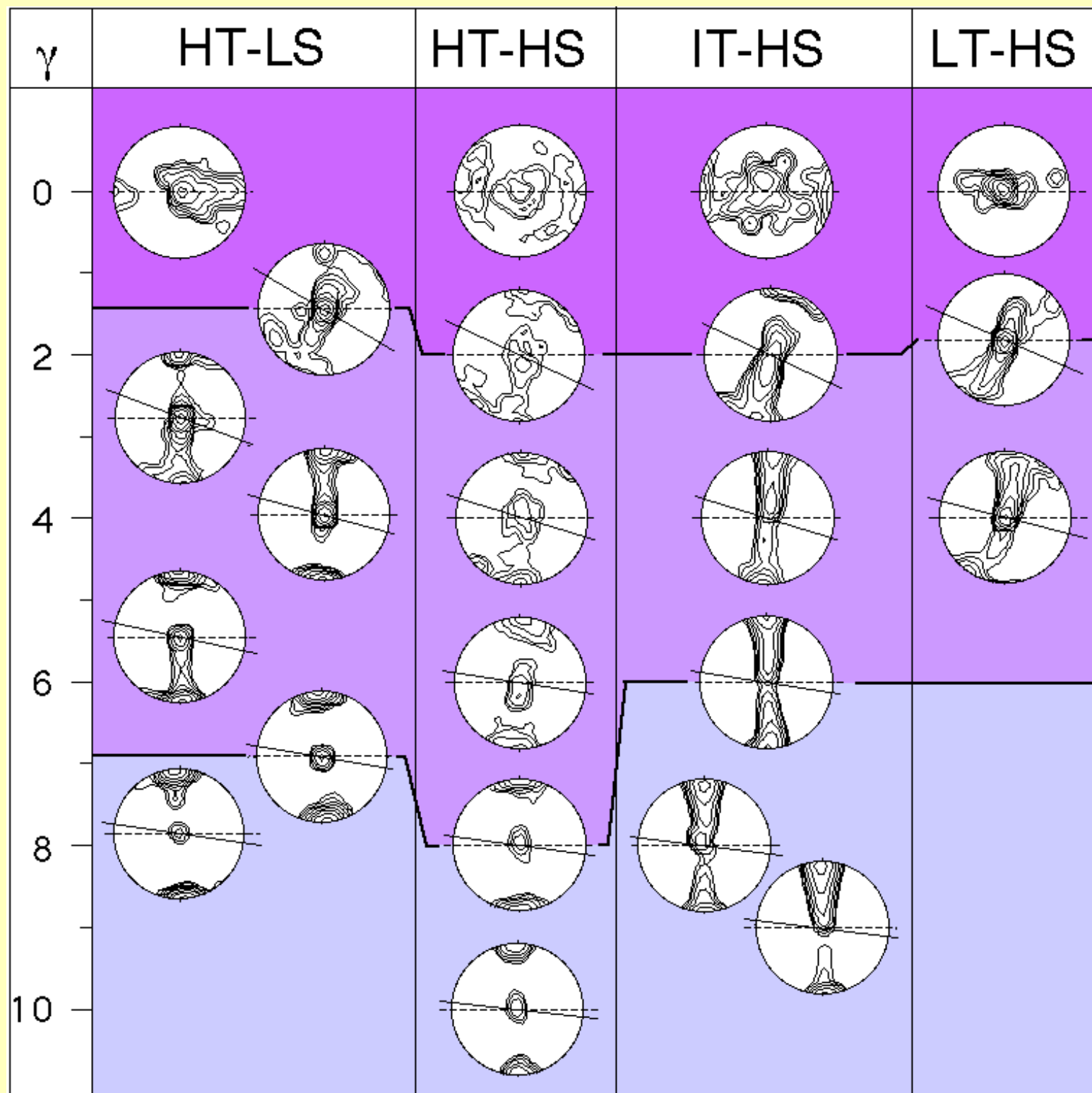
This figure shows that texture evolution at all experimental conditions comprises three different stages corresponding to stages of microfabric evolution:

1) During the first transient stage, a c-axis cross girdle develops which is symmetrically disposed with respect to the long axis of the finite strain ellipse (straight, black lines in the pole figures).

2) This c-axis cross girdle reduces to an oblique (with respect to the long axis of the finite strain ellipse) c-axis single girdle. In so doing, one of the two single girdles is eliminated.

3) The steady state textures are characterized either by two stable c-axis point maxima (HT-LS & HT-HS) or by a stable c-axis single girdle (IT-HS).

Grain size
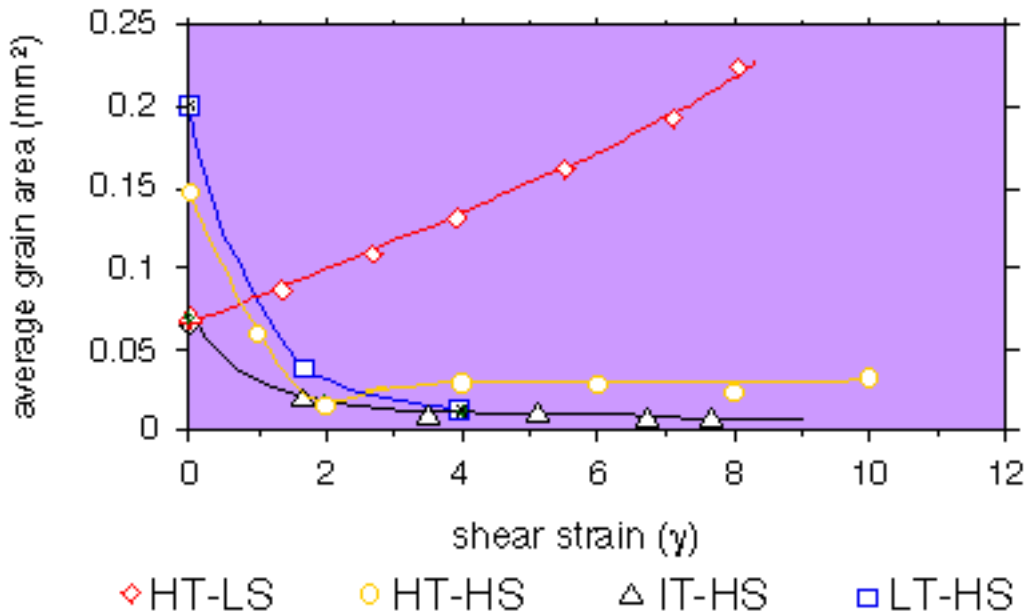
The average grain size is closely related to the strain rate and temperature-dependent assemblage of fabric modifying mechanisms.

A predominance of grain boundary migration recrystallization in the HT-LS experiments leads to a continuous increase in grain size, whereas grain size decreases in the IT-HS runs. This grain size reduction is related to subgrain rotation recrystallization. In the HT-HS experiments, subgrain rotation in the first transient stage is associated with grain size reduction, but intensified gbm during the second transient stage leads to grain growth.

Domain Width
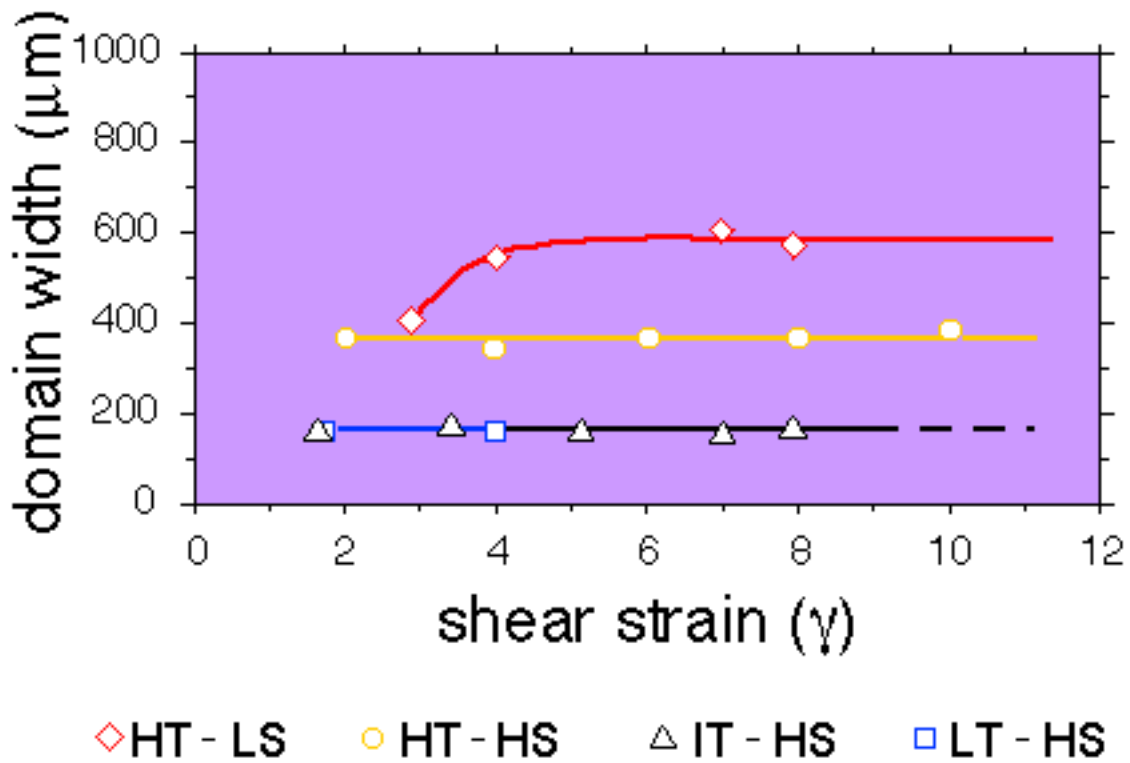
The domain width reflects directly the applied temperature / strain rate conditions: The higher the temperature and/or the lower the strain rate, the larger is the domain width.

Grain SPO
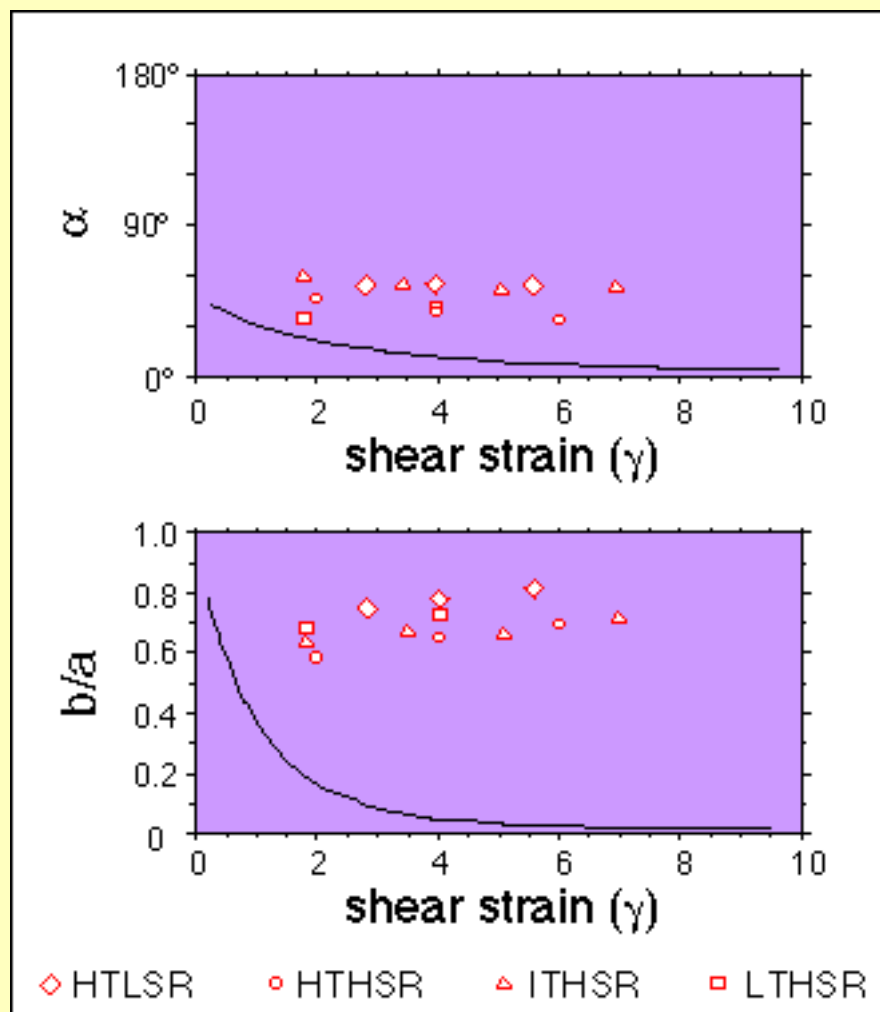
The upper diagram shows the orientation of grains´ long axes with increasing shear strain at different experimental conditions. The solid black line reflects the rotation path of the long axis of the finite strain ellipse.

A stable grain SPO at angles of 50-60° can be recognized in all experiments. Thus, the bulk SPO does not rotate above shear strains of 1.7 and all SPO's are more steeply oriented than the long axis of the finite strain ellipse.

In the lower diagram, the b/a (short/long) ratio of the grains is plotted against shear strain for the different experiments. The solid black line shows changes in axial ratios of the finite strain ellipse.

The b/a axial ratios of the grains are much larger than the those of the finite strain ellipse.

In light of these observations, the following question arises: By which mechanism is a steady state grain SPO preserved during continuous sample shearing?

Microfabric evolution
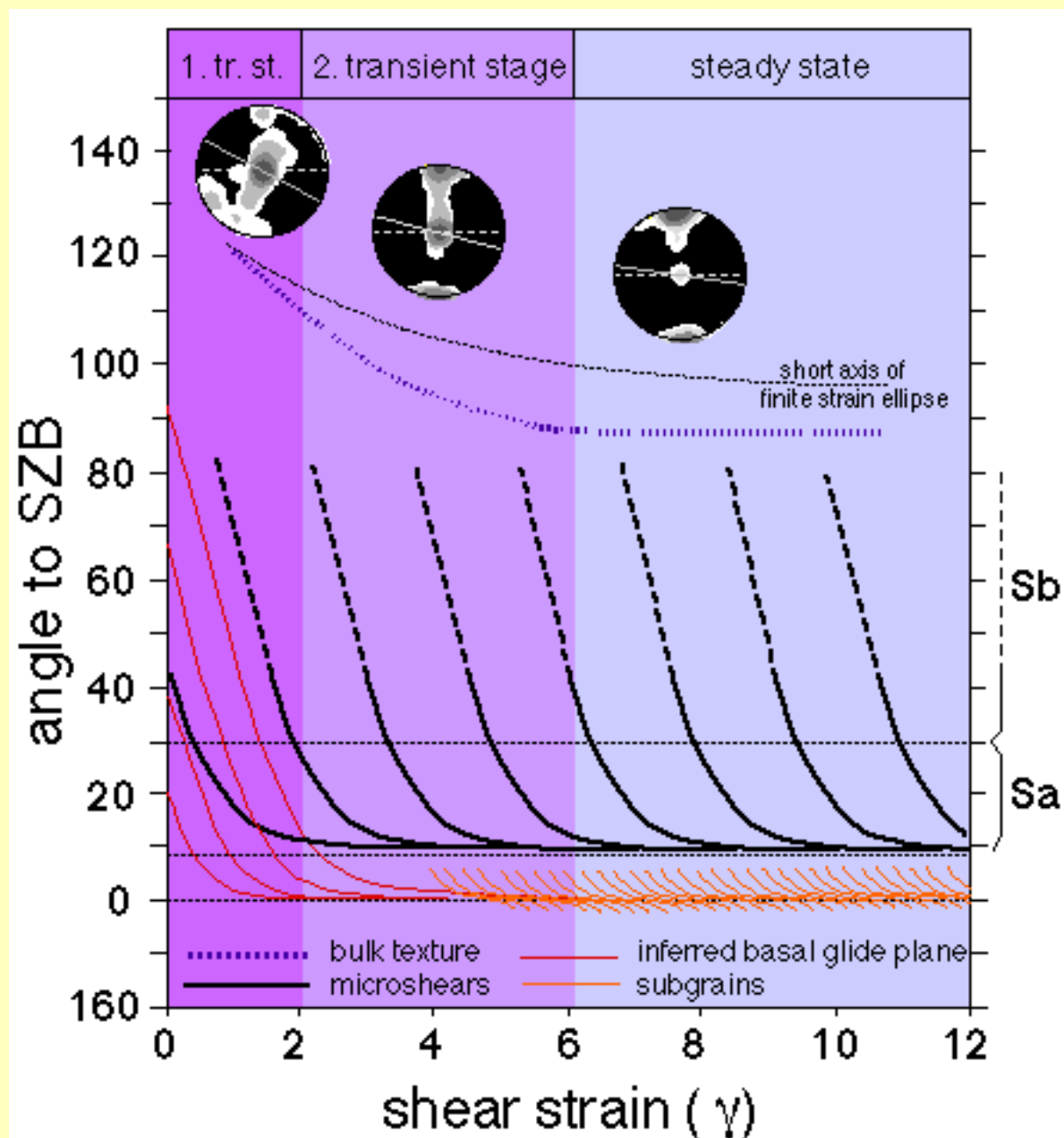
Irrespective of the experimental conditions applied, the following features are observed to accommodate strain irrespective of the temperature and strain rate conditions.

During the first transient stage, inter- and intracrystalline glide planes rotate into orientations for easy glide. This involves high rotation rates of microshears, individual c-axes and bulk textures.
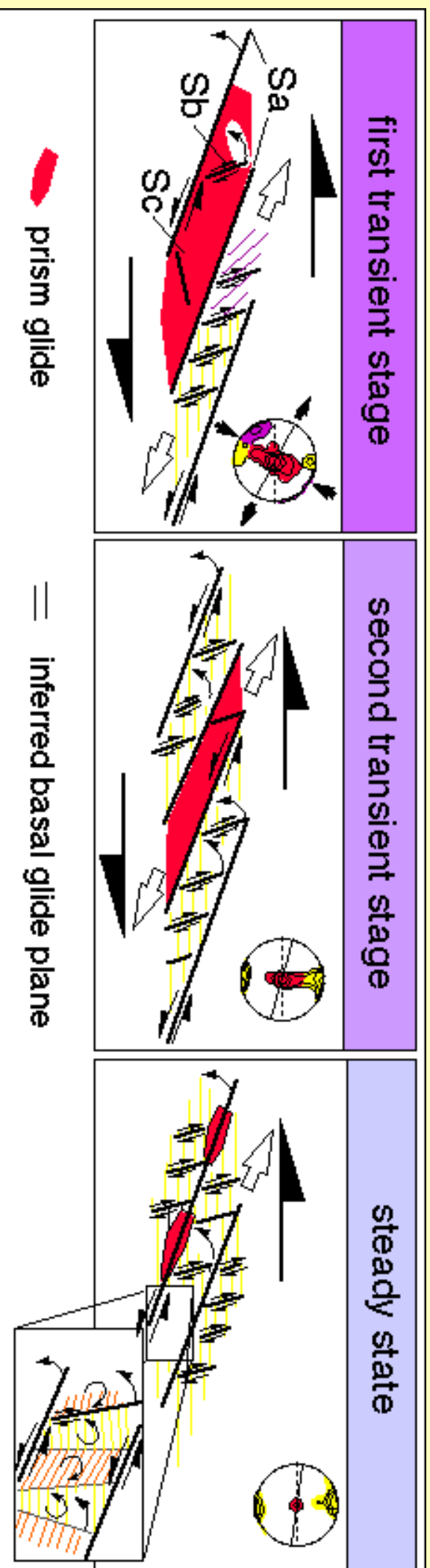
Rotation rates of individual c-axes and of the bulk texture decrease significantly during the second transient stage, while grain boundary migration recrystallization becomes more pronounced. Newly nucleated microshears with steep, Sb orientations and high rotation rates coexist with older microshears with a shallower Sa orientation and lower rotation rates.

The bulk texture is strain invariant at steady state, but deformation on the intra- to intergranular scale is heterogeneous. This involves the continuous nucleation, progressive rotation, and consumption of subgrains. Microshears with an Sa orientation are deactivated at very low angles to the SZB.

Differences in microfabric evolution (e.g. changes in area proportions of grains with specific crystallographic orientations and size) with strain rate and temperature mainly reflect the variations in

the relative activity of grain scale mechanisms (click HT-LS, HT-HS, IT-HS and LT-HS buttons).

Shear and rotation behaviour on different scales

first transient stage | second transient stage | steady state

prism glide

= inferred basal glide plane

At the end of the first transient stage, strain compatibility within the mylonite is maintained by a combination of microshearing, dynamic recrystallization, and inter- and intracrystalline gliding. The symmetry of the c-axis cross girdle suggests that the basal glide planes are in a conjugate orientation with respect to the instantaneous stretching direction. The Sb- and Sc-oriented microshears are also symmetrically oriented with respect to this direction. Thus, both intergranular microshearing and intragranular gliding on the basal planes accommodate strain by allowing the material to elongate in the direction of greatest instantaneous stretching.

The consumption of grains less favorably oriented for intracrystalline gliding leads to an increase in the volume of grains whose basal planes are oriented subparallel to the SZB. Therefore, a domainal microfabric develops during the second transient stage consisting of yellow and magenta domains. At this stage, grain boundaries and domain boundaries coincide, respectively, with Sb and Sa microshears. Thus, sample elongation results from a close interaction of Sb-oriented microshears and basal gliding, whereas the Sa-oriented microshears accommodate the differences in the rate and amount of shear strain between the different domains.

At steady state, most of of the grains' basal planes are oriented subparallel to the SZB. Closer examination of individual grains reveals that the c-axes of subgrains continuously rotate, and so accommodate different amounts of shear strain with different local strain rates. Consequently, microshears are required to maintain strain compatibility between the different subgrains and grain aggregates. As in the second transient stage, a combination of basal gliding subparallel to the SZB and shearing along the Sb-oriented microshears maintain compatibility in the direction of greatest instantaneous stretching, whereas the Sa-oriented microshears accommodate strain between the different domains.

Glossary Microfabric ← →

Steady state of microfabric elements
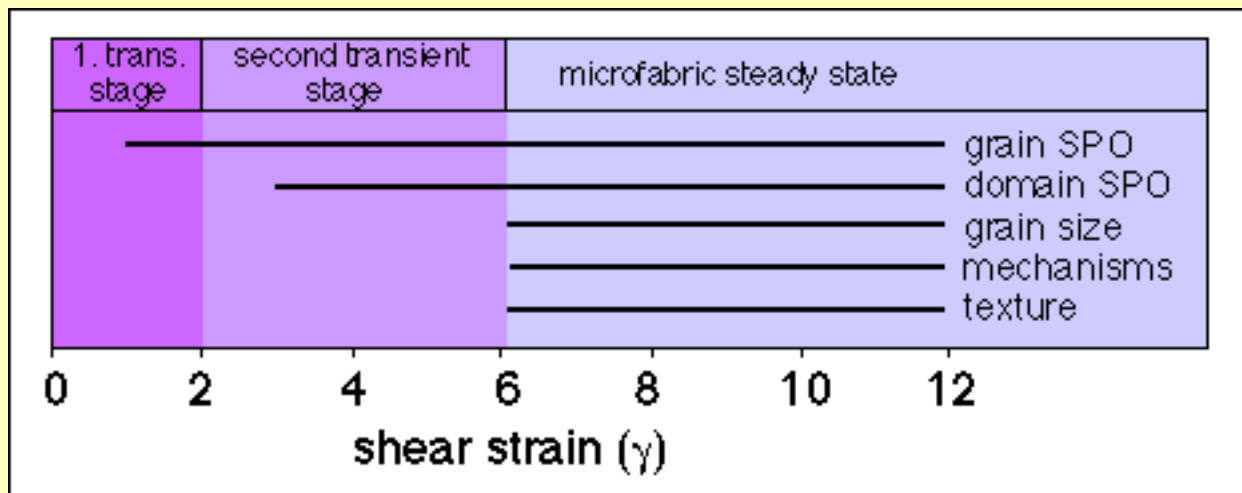
Different microfabric elements attain steady state at different strains. Grain SPO attains steady state at shear strains of 1.5 and above, closely followed by the development of a stable domainal SPO at shear strains of about 3 and above. The last elements to attain steady state are grain size, fabric modifying mechanism assemblage and bulk texture. This confirms previous studies indicating that late changes in the strain field may be recorded in the grain or domainal SPOs of the microfabric, whereas texture and grain size reflect an older part of deformation history.

HT-HS CPO area
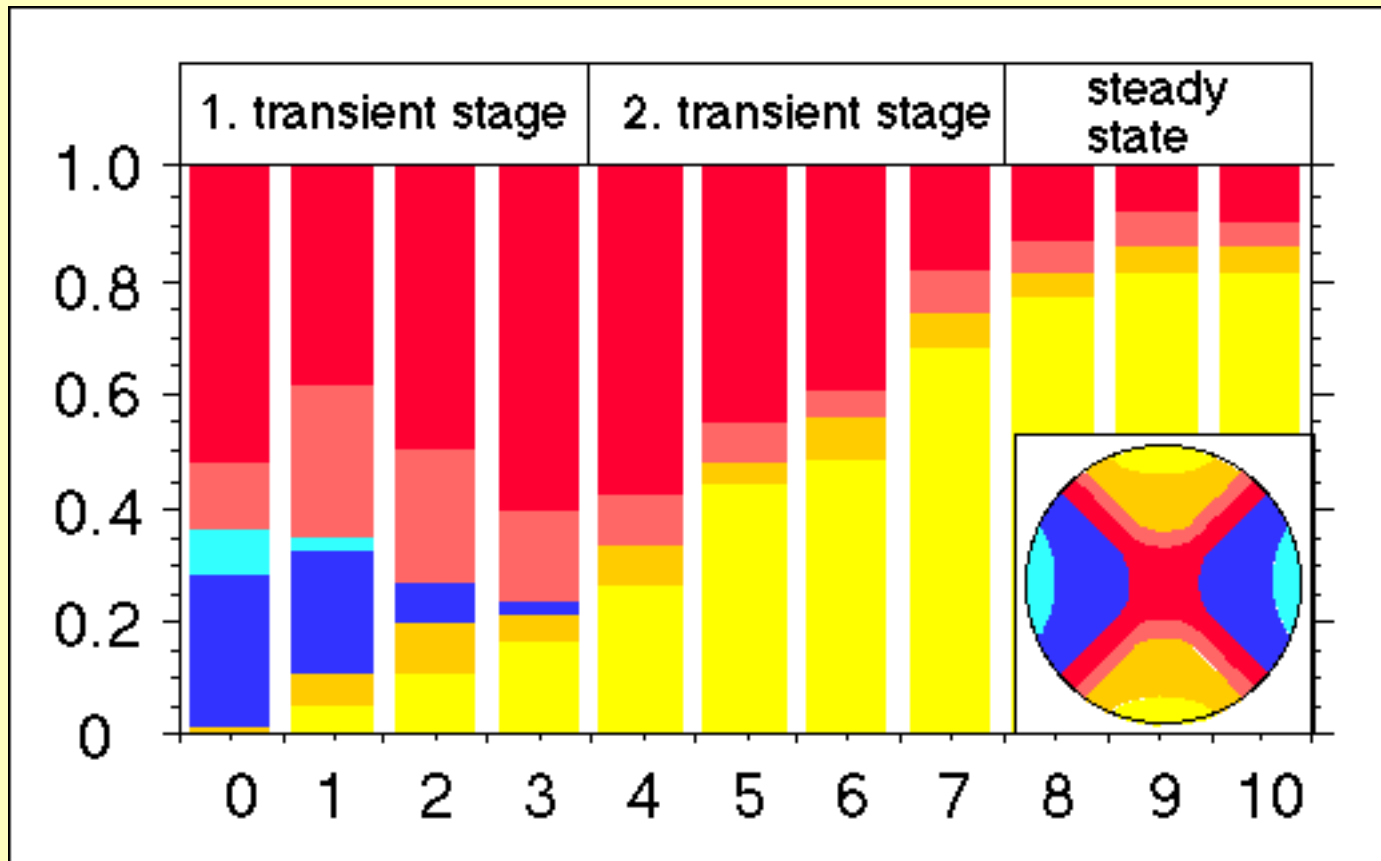
Grains with crystallographic orientations corresponding to a blue colour disappear, whereas the volume proportion of yellow grains increases.

During the second transient stage, the volume proportion of yellow grains increases at the expense of that of the magenta grains.

At steady state, the volume proportions of yellow and magenta grains is strain invariant.

HT-HS Deformation Mechanism Activity
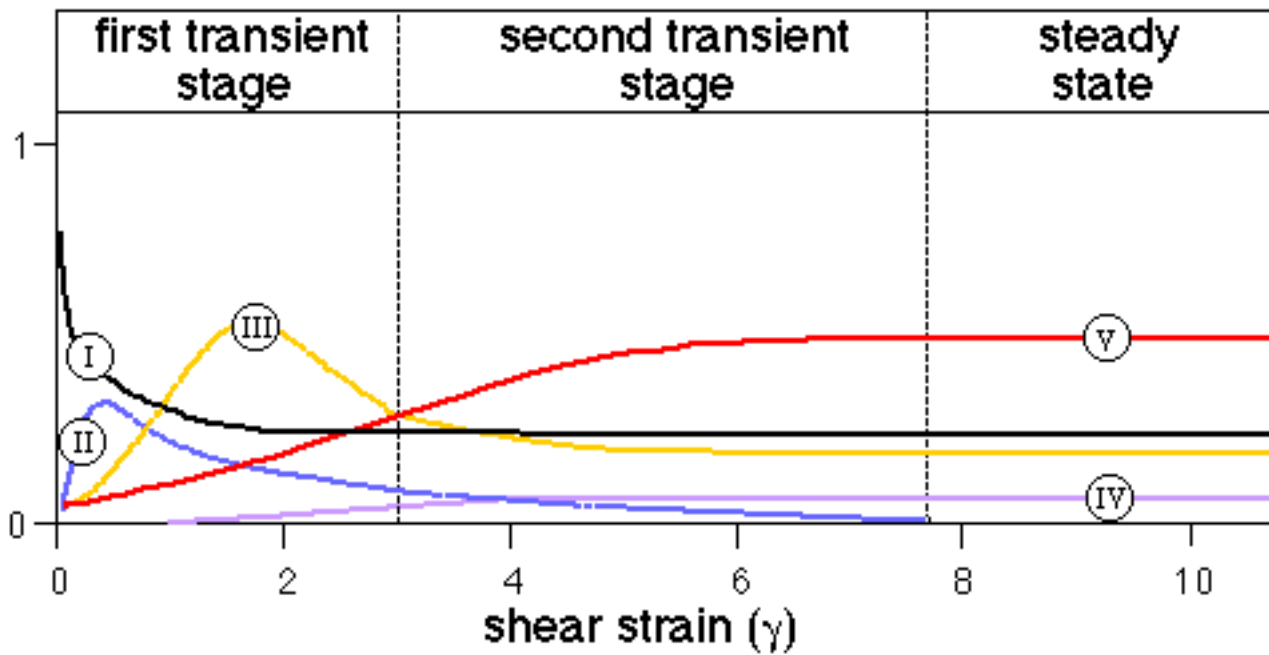
During the first transient stage microfabric is primarily influenced by rotational mechanisms (glide induced vorticity, subgrain rotation, rigid body rotation).

Grain boundary migration recrystallization shows a strong influence on microfabric in the second part of the HT-HS experiments.

Steady state microfabric is preserved by a combination of gbm, glide induced vorticity, subgrain rotation and spontaneous nucleation.

HT-HS Textures

As a consequence of sample preparation, the c-axes of the initial texture centre of the pole figure.

At the end of the first transient stage ($0<\gamma<2$) a c-axis cross girdle develops which is symmetrically disposed with respect to the long axis of the finite strain ellipse (= rotating black line outside the pole figure).

During the second transient stage ($2<\gamma<8$) the former c-axis cross girdle reduces to an oblique c-axis single girdle. With strain, c-axis concentration at the periphery of the pole figure strengthens resulting in the formation of two c-axis point maxima.

The positions and intensity of the two c-axis point maxima are strain invariant at steady state ($\gamma>8$).
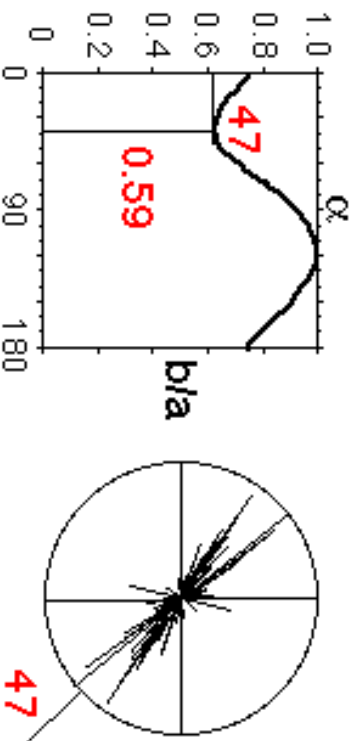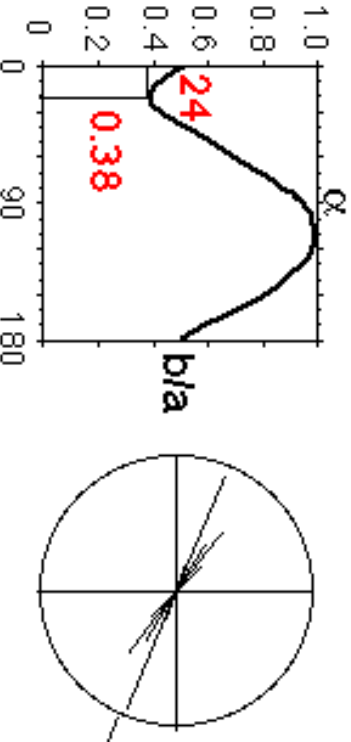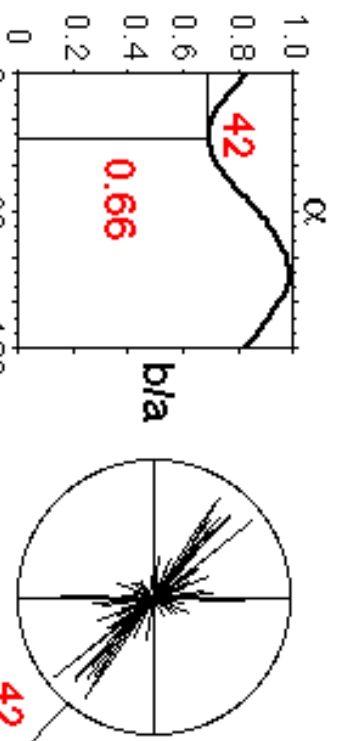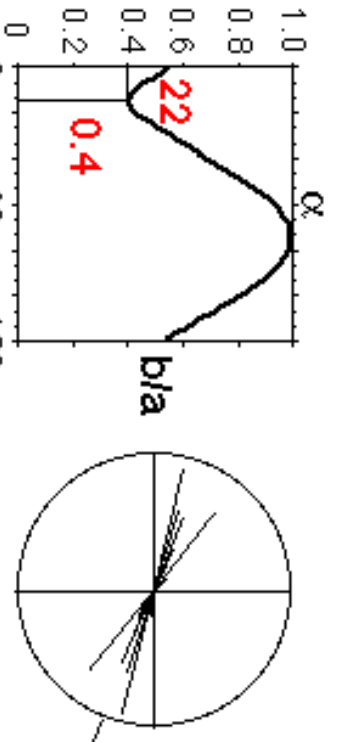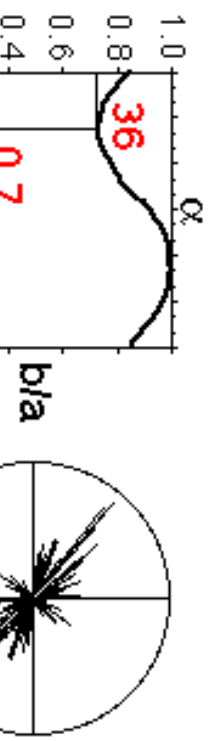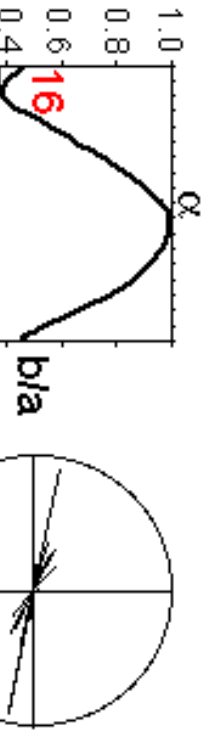
The formation of these strong textures indicates that dislocation creep is the main deformation mechanism which is active during the entire experiment.
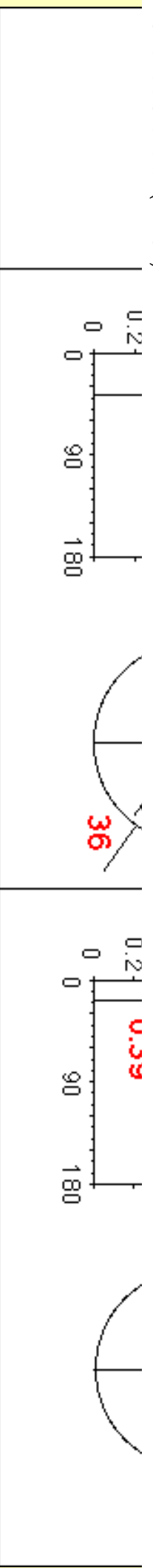
HT-HS Grain Size

As a consequence strong component of subgrain rotation during the first transient stage, the average grain area significantly decreases.

With strain, however, intensified contribution of gbm to microfabric evolution results in an increase of the average grain area.

# HT-HS Particle Orientation (PAROR)

HT-HS

grains	domains

$\gamma = 2$ — grains: 47, 0.59 — domains: 24, 0.38

$\gamma = 4$ — grains: 42, 0.66 — domains: 22, 0.4

$\gamma = 6$ — grains: 36, 0.7 — domains: 16

The long axes of grains show inclinations of about 36-47° with respect to the SZB. The grain b/a ratios are smaller than in the HT-LS experiments.

In comparison to the grain SPO, the domains have lower b/a ratios and their SPO's show an inclination of about 16-24° with respect to the SZB.

Glossary | Experiments | HT-LS | HT-HS | IT-HS | LT-HS | ← | →

HT-LS CPO Area
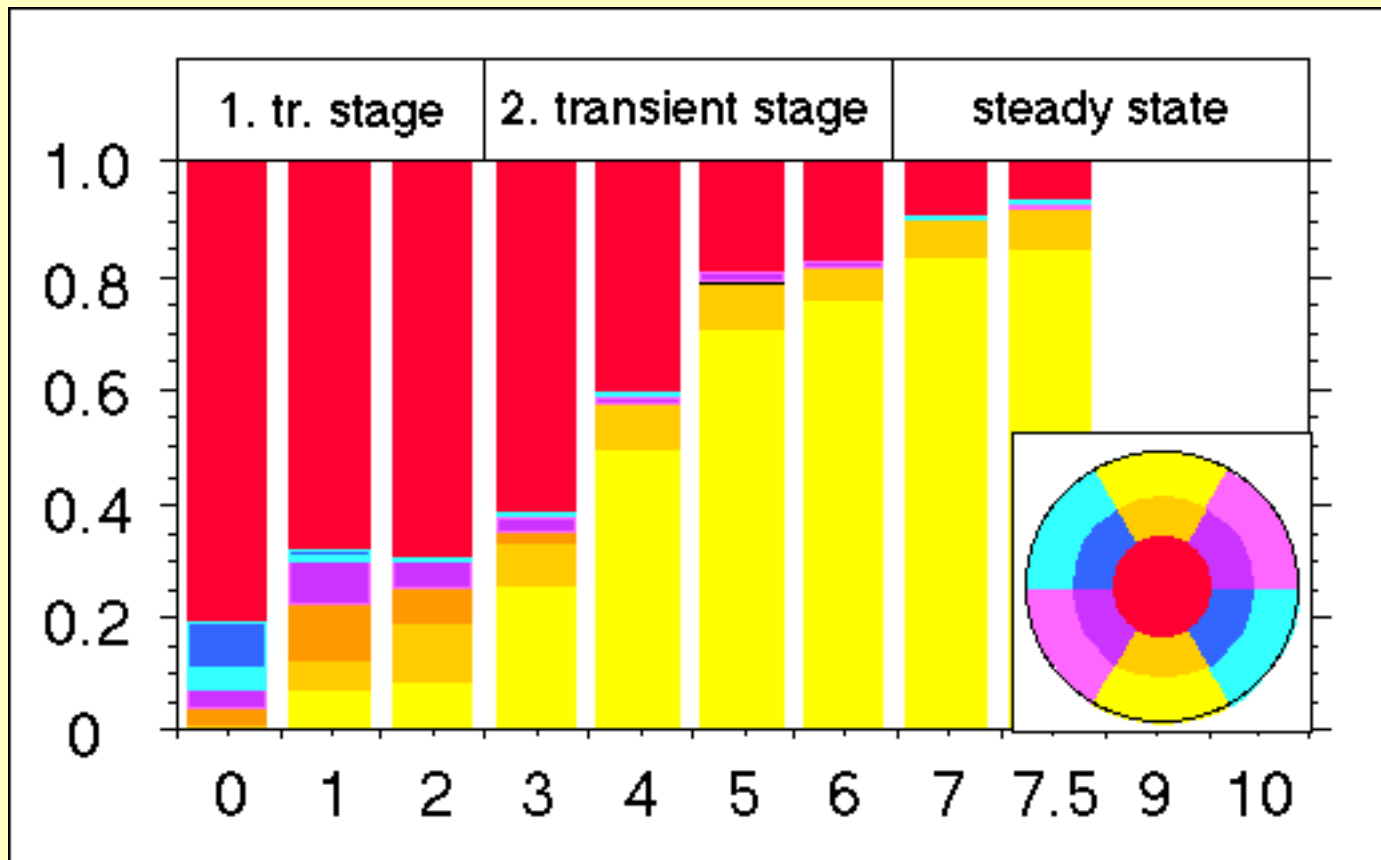
This diagram shows changes in the areal proportions of grains with a specific crystallographic orientation (vertical axis) as a function of shear strain (horizontral axis). The crystallographic orientations of the grains are colour coded (pole diagram at lower right hand corner).

Grains with orientations corresponding to blue and violet interference colours are eliminated, whereas areal proportion of yellow grains increases.

The increase in volume proportion of yellow grains is greatest during the second transient stage, whereas at steady state the areal proportion of yellow and magenta grains remains constant with strain.

HT-LS Deformation Mechanism Activity
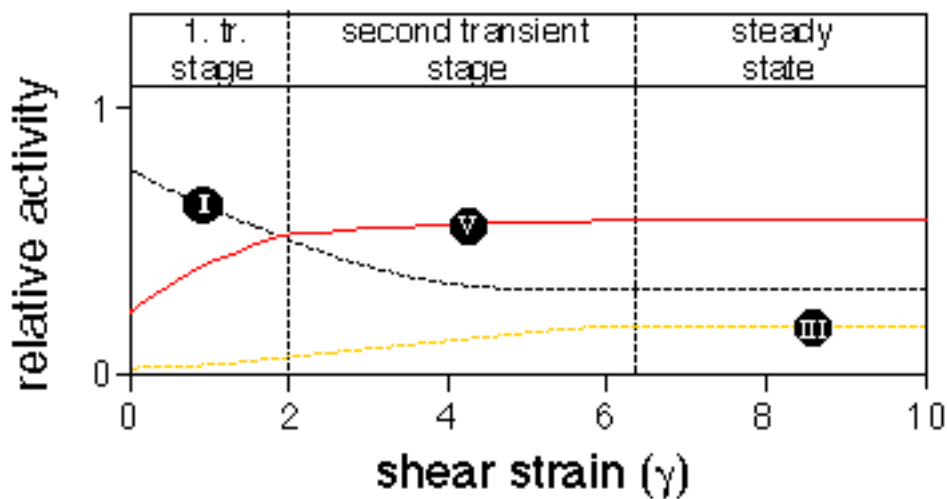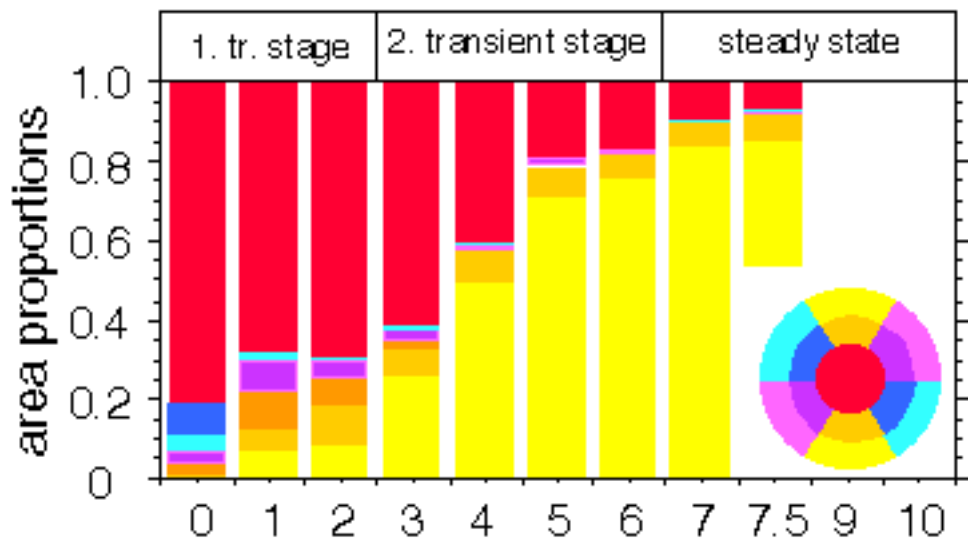
Glide induced vorticity is the principal rotation mechanism during the first transient stage.

In the second transient stage influence of grain boundary migration on microfabric evolution increases whereas the rotational mechanism only slightly modify the microfabric.

At steady state microfabric is preserved by a combination of grain and subgrain boundary migration, glide induced vorticity and subgrain rotation.

Glossary Experiments HT-LS HT-HS IT-HS LT-HS ← →

HT-LS Textural Evolution

As a consequence of sample preparation, the C-axes of the initial texture concentrate around the Y-fabric direction.

At the end of the first transient stage ($0<\gamma<1.5$) a c-axis cross girdle develops which is symmetrically disposed with respect to the long axis of the finite strain ellipse (see rotating black line outside the pole figure).

During the second transient stage ($1.5<\gamma<6$) the former c-axis cross girdle reduces to an oblique c-axis single girdle. With strain, c-axis concentra-
tion at the periphery of the pole figure strengthens resulting in the formation of two c-axis point maxima.

The positions and intensity of the two c-axis point maxima are strain invariant at steady state ($\gamma>6$).

The formation of these strong textures indicates that dislocation creep is the main deformation mechanism which is active during the entire experiment.

HT-LS Grain Size

The average grain area increases during the entire experiment due to on going activity of grain boundary migration recrystallization.
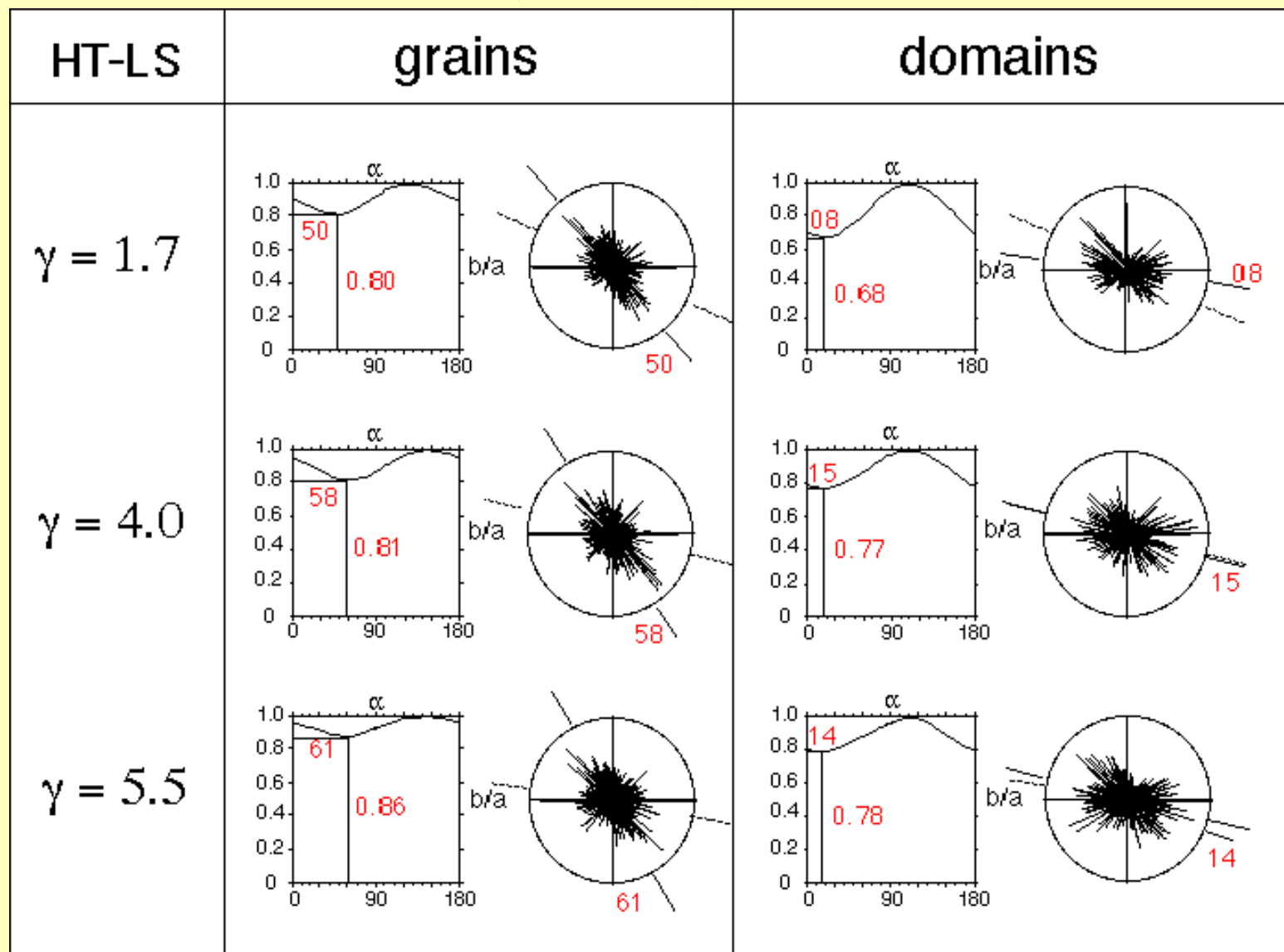
HT-LS Particle Orientation (PAROR)
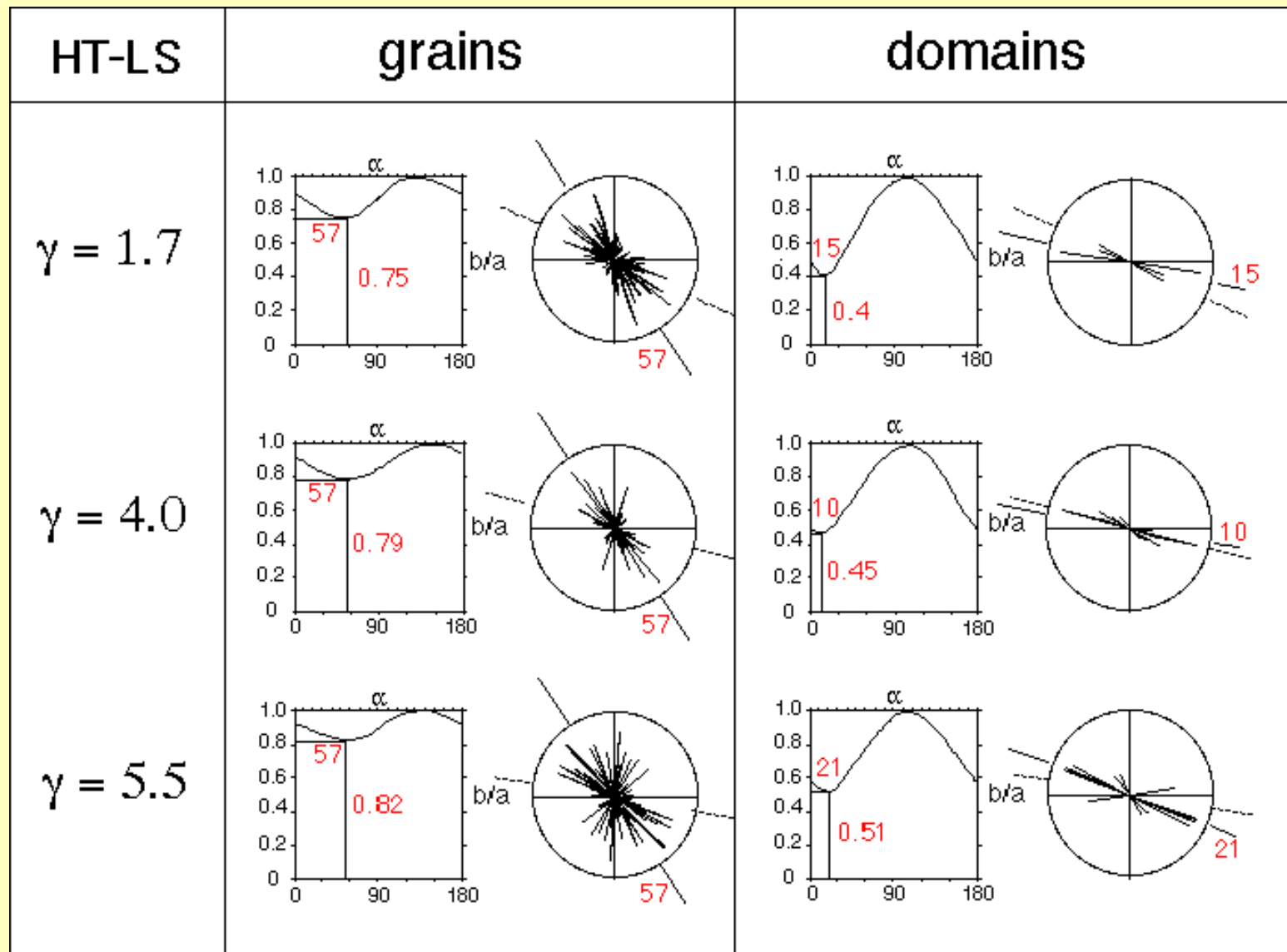
The long axes of grains show inclinations of about 57° with respect to the SZB. The grain b/a ratios are in the range of 0.75 - 0.82.

In comparison to the grain SPO, the domains have lower b/a ratios and their SPO's show an inclination of about 10-21° with respect to the SZB.

HT-LS Surface Orientation (SURFOR)

HT-LS	grains	domains
$\gamma = 1.7$		
$\gamma = 4.0$		
$\gamma = 5.5$		

Similar to the grain SPO the grain surface SPOs show a steep inclination at angles of 50-61° with respect to the SZB.

The domain surface SPO's have inclinations between 8-14° with respect to the shear zone boundary.

HT-LS Strain

Although deformation takes place within the entire area between the frosted grips, the moderately to highly strained regions concentrate along the lower SZB during the first part of the experiment. At higher shear strain, however, the trace of the intermediate to high strain zones tends to connect with the upper left corner of the analogue sample showing a diagonal arrangement.

In contrast, the highest strained parts (orange to red contour intervals) of the sample show always an enechelon-like oblique orientation with respect to the SZB.

HT-LSHigh Strain Zone Evolution

This diagram presents grain boundary outlines of the high strain zones shown on the previous page. Two types of high strain zones can be distinguished: (a) relative long high strain zones at angles of 20-50° with respect to the SZB and (b) shorter high strain zones with inclinations of 50-80° with respect to the SZB. Note that this general strain distribution pattern is preserved over the entire experiment.

The changes in positions of intermediately to highly strained parts is nicely reflected by the highest still interconnected contour interval.

IT-HS CPO area
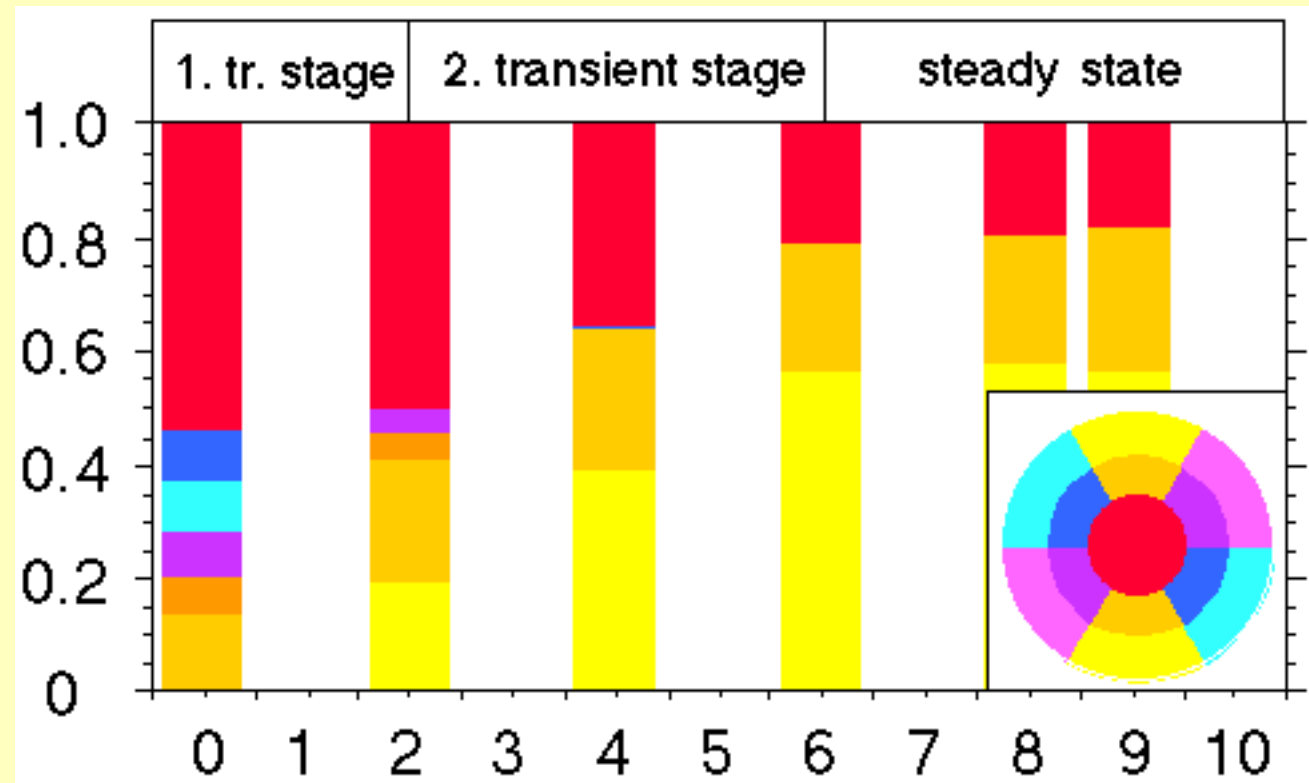
Subgrain rotation and grain boundary migration recrystallization are associated with a significant increase in areal proportions of yellow grains. Above shear strains of six, the areal proportions of yellow and magenta grains are strain invariant. This is diagnostic of steady state.

IT-HS Deformation Mechanism Activity
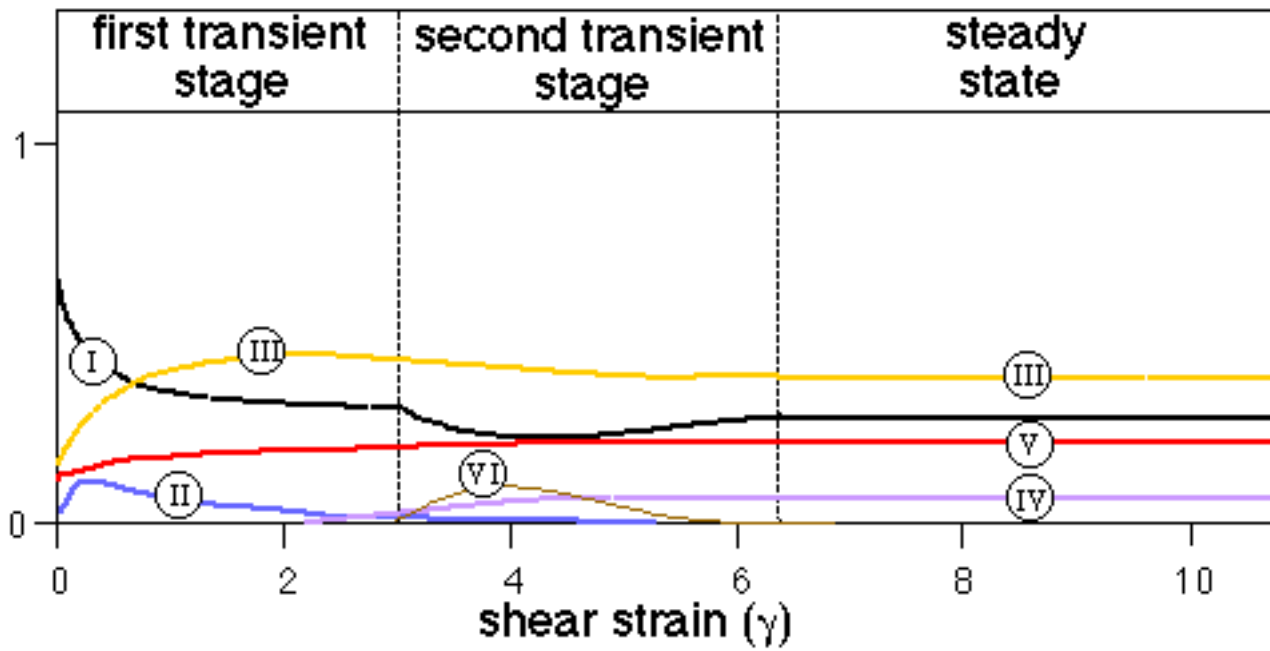
Subgrain rotation and glide induced vorticity are the main rotational mechanisms during the first transient stage.

The combination of subgrain rotation, gbm and glide induced vorticity accommodate deformation during the second transient stage. The appearance of some small cracks indicates that fracturingadditionally contributes to bulk deformation.

The steady state mechanism assemblage comprises subgrain rotation, gbm and glide induced vorticity.

IT-HS Textures

As in the experiments before, the c-axes initially concentrate around the Y-fabric direction.

During the first transient stage a symmetric c-axis cross girdle develops which reduces to an oblique single girdle with increasing shear strain (second transient stage).

In contrast to the high temperature experiments the steady state texture comprises a stable c-axis single girdle instead of c-axis point maxima.

IT-HS Grain Size

High and continuous activity of subgrain rotation recrystallization reduces the average grain size becoming stable at steady state.
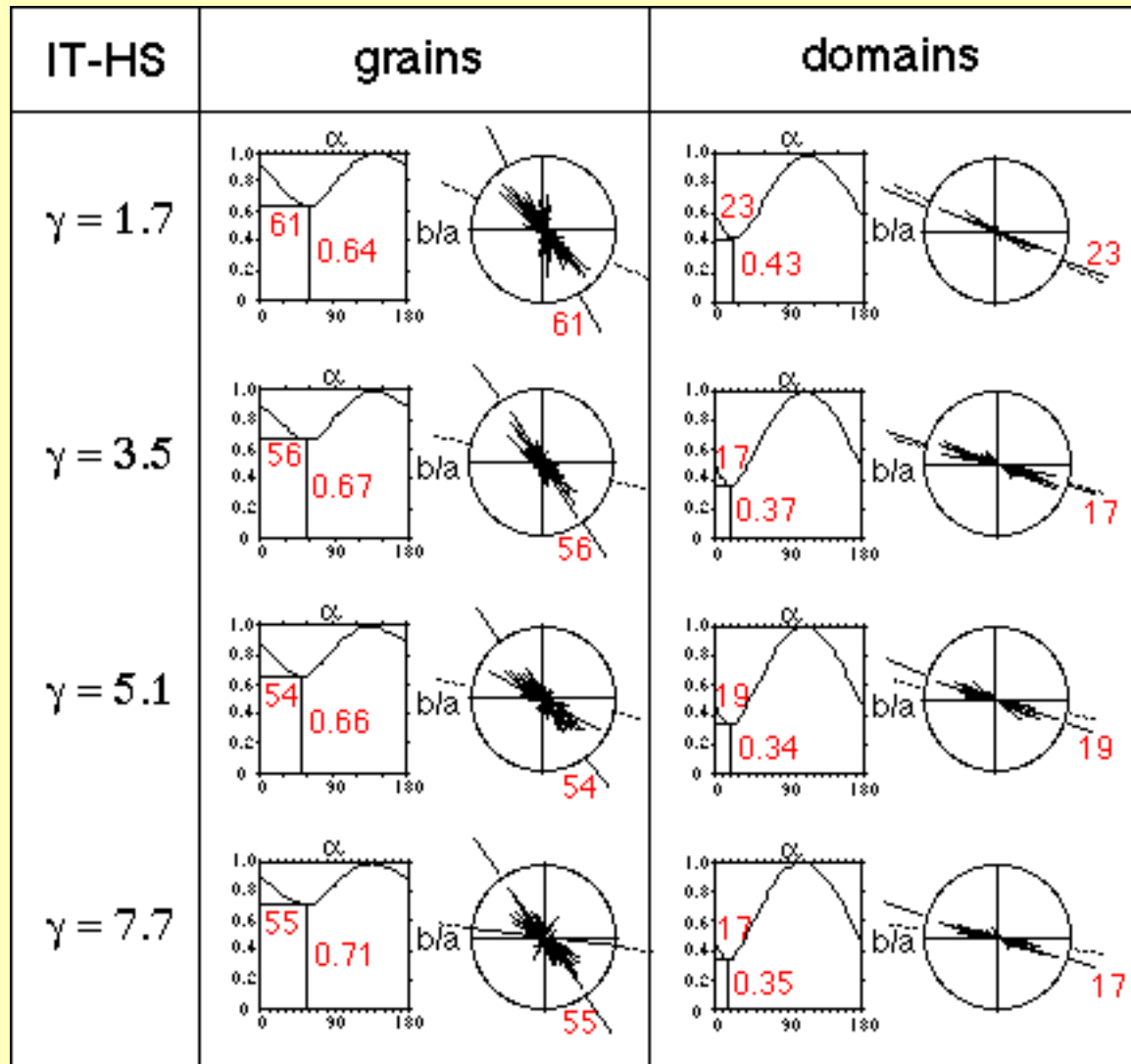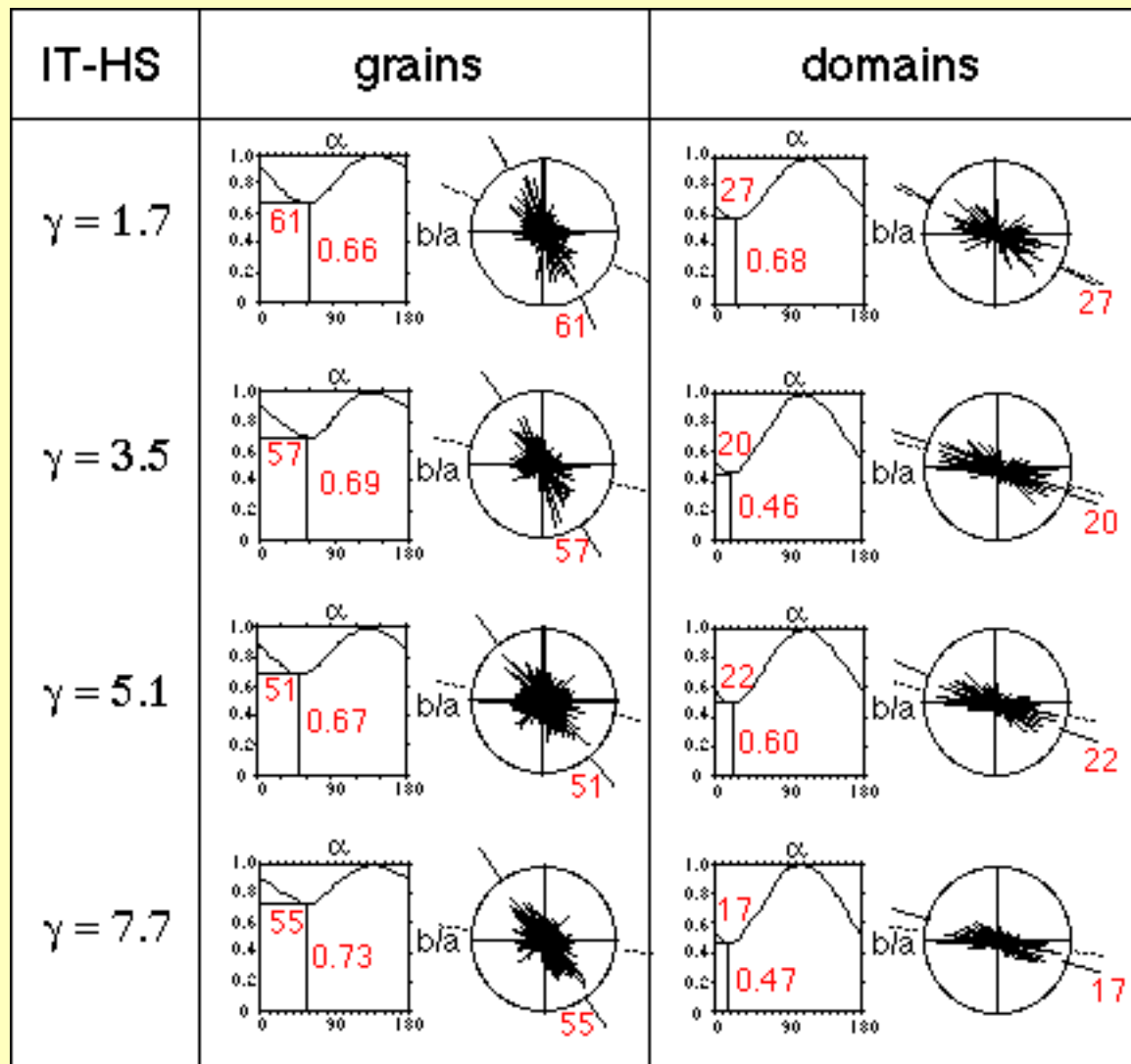
IT-HS Grain Size

High and continuous activity of subgrain rotation recrystallization reduces the average grain size becoming stable at steady state.

IT-HS Particle Orientation (PAROR)

IT-HS	grains	domains
$\gamma = 1.7$	61 0.64 b/a 61	23 0.43 b/a 23
$\gamma = 3.5$	56 0.67 b/a 56	17 0.37 b/a 17
$\gamma = 5.1$	54 0.66 b/a 54	19 0.34 b/a 19
$\gamma = 7.7$	55 0.71 b/a 55	17 0.35 b/a 17

Above shear strains of 1.7 the grain SPO is in steady state at angles of about 54-61° with respect to the SZB. The grain b/a ratio (0.64-0.71) is smaller than in the high temperature experiments.

At shear strains above 3.5 domains show stable SPOs at angles of 17-19° with respect to the SZB. The domainal steady state b/a ratios (0.34-0.37) are slightly smaller than in the high temperature experiments.

IT-HS Surface orientation (SURFOR)

The surface SPO of grains shows inclinations between 51° and 61°. In contrast to the high temperature experiments, the b/a ratios (0.73-0.66) of the IT-HS grains are smaller.

The inclinations of the surface SPOs of the domains are between 17° and 27°.

IT-HS Strain

In this type of experiments the moderately to highly strained parts tend to concentrate along the lower SZB and the upper SZB at the beginning and the end of deformation, respectively.

Again the highest strained parts are obliquely oriented with respect to the SZB.

IT-HS Shear Zone Evolution

This diagram presents grain boundary outlines of the high strain zones shown on the previous page. Two types of high strain zones can be distinguished: (1) relative long high strain zones at angles of 20-50° with respect to the SZB and (2) shorter high strain zones with inclinations of 50-80° with respect to the SZB. Note that this general strain distribution pattern is preserved over the entire experiment.

The aforementioned changes in positions of intermediate to high strain zones can be observed by the traces of the highest still interconnected contour interval.

LT-HS CPO area
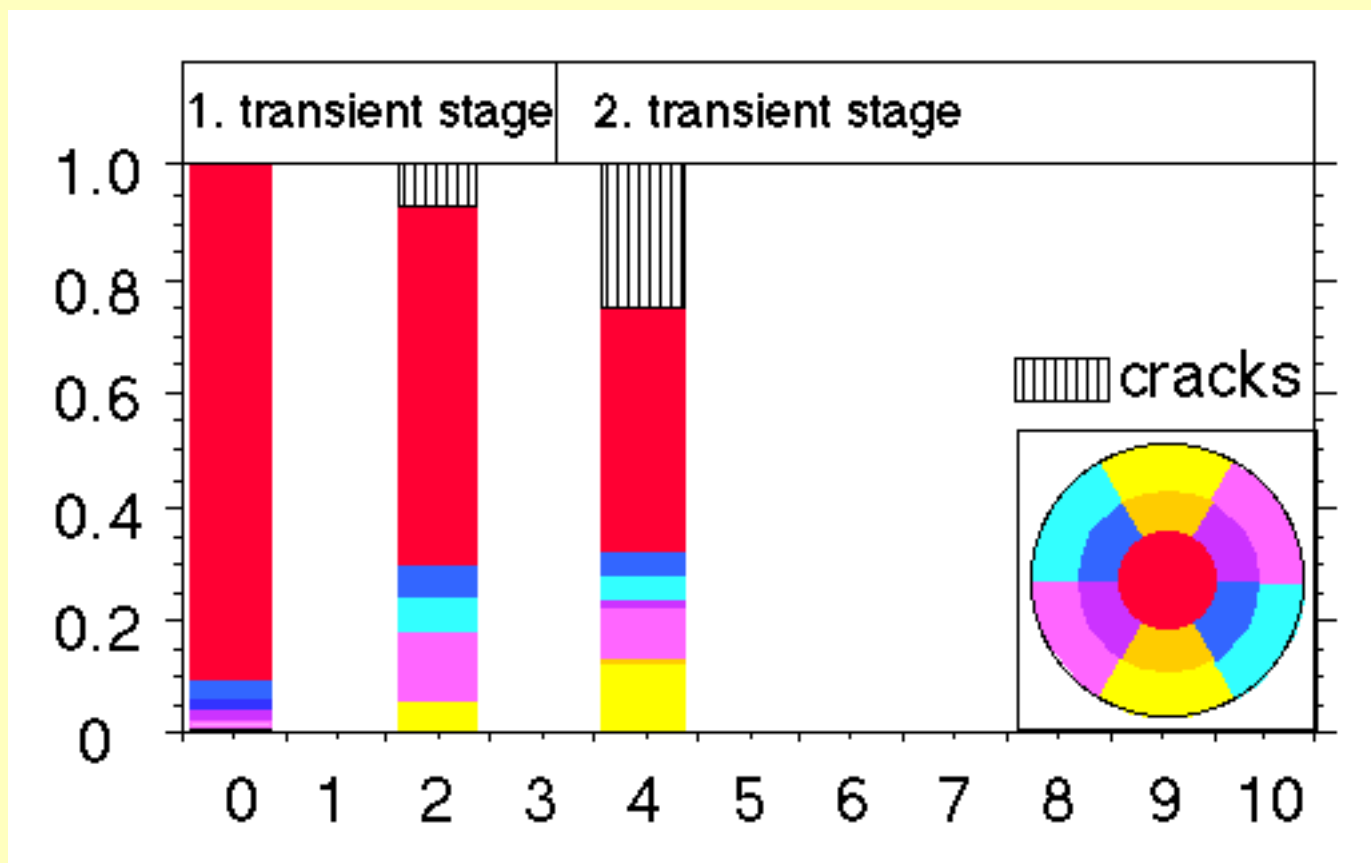
Although the areal proportion of yellow grains increases, the rate at which this proportion increases (per increment of shear strain) is much lower than in the other experiments.

LT-HS Deformation Mechanism Activity
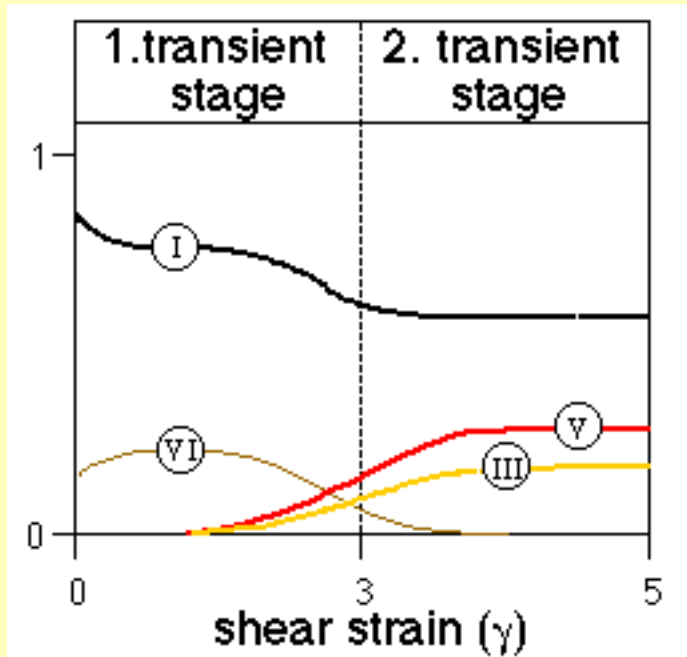
Under these experimental conditions crystal plasticity and dynamic recrystallization are not able to maintain strain compatibility. Therefore, fracturing is additionally activated to accommodate strain during the first transient stage.

In the second transient stage dynamic recrystallization (gbm, subgrain rotation) become more pronounced whereas the activity of fracturing reduces.

LT-HS Textures

Although fracturing plays an important role during the LT-HS experiments the development of a texture indicates a strong activity of crystal plastic processes.

At the end of the first transient stage the texture comprises a sort of a c-axis cross girdle which reduces to an oblique c-axis single girdle during the second transient stage.
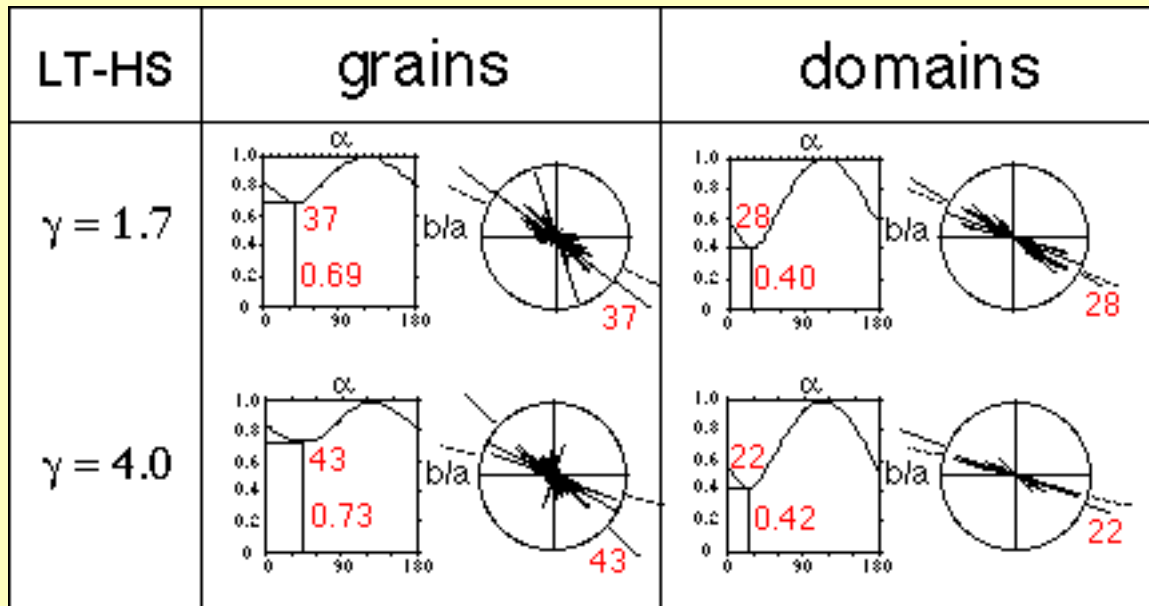
LT-HS Grain Size

As a consequence of simultaneous activity of gbm, subgrain rotation and fracturing, the average grain area continuously decreases.

LT-HS Particle orientation (PAROR)

LT-HS	grains	domains
$\gamma = 1.7$	37 0.69	28 0.40
$\gamma = 4.0$	43 0.73	22 0.42

The grains long axis shows an average inclination of 69-73° and b/a ratios of 0.69-0.73.

Domains are again less steep oriented (22-28°) and have much smaller b/a ratios (0.4-0.42).

Glossary | Experiments | HT-LS | HT-HS | IT-HS | LT-HS | ← | →

LT-HS Surface orientation (SURFOR)

LT-HS	grains	domains
$\gamma = 1.7$	38 / 0.78	29 / 0.56
$\gamma = 4.0$	42 / 0.75	24 / 0.63
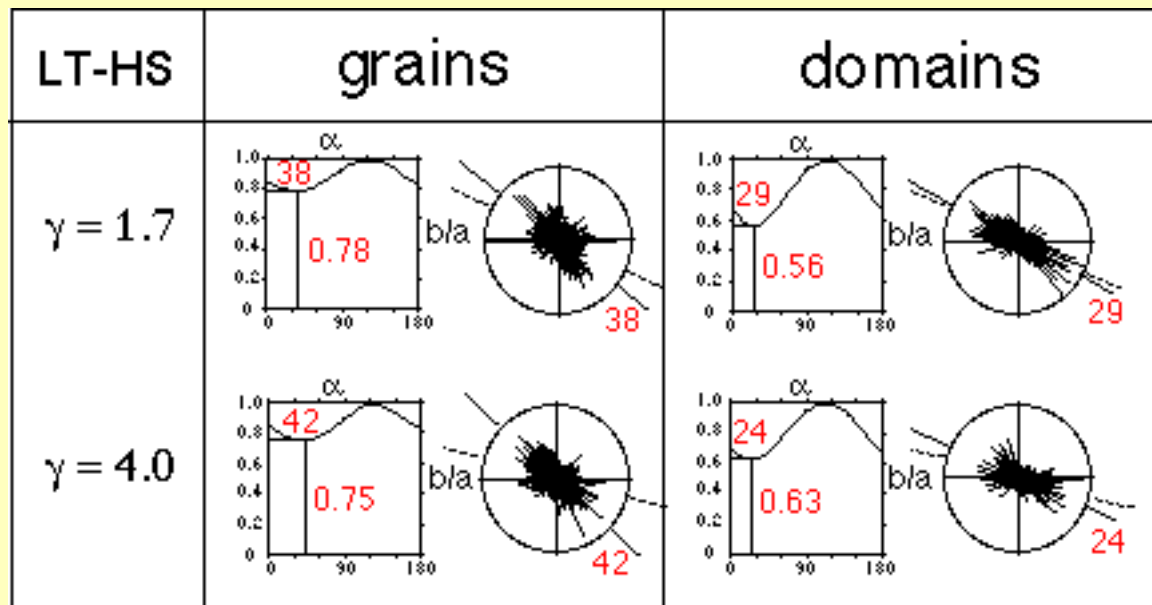
Although the grain b/a ratios are relatively high (0.75-0.78), the grain surface SPOs (37-42°) are less steep inclined than in the high and intermediate temp. experiments.

The average orientation of the domains surface segments reflects an angle of 24-29° with respect to the SZB.

LT-HS Strain

Under low temperature conditions material failure is required to maintain strain compatibility. The resulting fractures control the trace of the moderate to high strain zones (see $\gamma = 4$).

Although fracturing is active, the highest strained parts are again obliquely oriented with respect to the shear zone boundary.

LT-HS Shear Zones

Similar to the HT-LS and IT-HS experiments two sets of high strain zones can also be observed under the low temperature conditions: (1) relative long high strain zones at angles of 20-50° with respect to the SZB and (2) shorter high strain zones with inclinations of 50-80° with respect to the SZB.